

# Development of Recycling Process of Photovoltaic Ribbon in Spent Solar Module using Water Vapor Generated by Waste Heat

Jin-Seok Lee<sup>1</sup>, Bo-Yun Jang<sup>1</sup>, Joon-Soo Kim<sup>1</sup>, Young-Soo Ahn<sup>1</sup>, Gi-Hwan Kang<sup>2</sup>  
and Jei-Pil Wang<sup>\*3</sup>

<sup>1</sup>Advanced Materials and Devices Laboratory, Korea Institute of Energy Research, Daejeon 305-343, Korea

<sup>2</sup>Photovoltaic Laboratory, Korea Institute of Energy Research, Daejeon 305-343, Korea

<sup>3</sup>Department of Metallurgical Engineering, Pukyong National University, Busan 608-739, Korea

\*Corresponding author, email: jpwang@pknu.ac.kr

New recycling process was attempted to recover copper substrate and to remove coating layer consisting of tin (Sn) and lead (Pb) of photovoltaic ribbon in spent solar module by means of oxidation using water vapor generated by waste heat. The oxidation behavior of the photovoltaic ribbon was studied under two different conditions of dry and moist atmosphere. The rate of oxidation was compared at 500°C in given conditions and the oxidized coating layer consisting of lead of 68.99wt% and tin of 31.21wt% was taken off from the substrate at room temperature. The chemical composition of copper ribbon after oxidation was analyzed using ICP-MS (Inductively Coupled Plasma Mass Spectrometry) and the purity of copper obtained was found to be about 99.5wt%. Further process using zone-melting furnace was consequently carried out fabricate high-purity copper and 4N grade of copper ( $\geq 99.99\%$ ) was finally obtained. The component of coating layer was safely stabilized as oxide forms of PbO and SnO.

Keywords: *Photovoltaic Ribbon, Oxidation, Water Vapor, Zone Melting, Copper*

## 1. Introduction

The increased energy consumption of recent industrial advancements has further increased the use of fossil energy, resulting in serious environmental problems and a growing concern over energy depletion. A great deal of research has been devoted to the development of new and renewable energy sources to solve these problems. In particular, the solar energy industry has prompted rapid growth of photovoltaic energy research.<sup>1)</sup> Unlike fossil fuels, photovoltaic cells are ecofriendly, powered by a renewable energy source, and have a lifetime of 15 years or more; as a result of these traits, their development is rapidly growing on the national and global scales.<sup>2)</sup>

With the growth of the solar energy industry, the volume of spent photovoltaic modules has continued to increase, with its cumulative volume estimated to reach about 130,000tons by the year of 2030. However, over 90% of the end-of-lifetime photovoltaic modules can be recycled, despite currently being buried in general landfills or completely neglected.<sup>3)4)</sup> For this reason, various studies have been carried out on the recovery and recycling of precious resources from spent photovoltaic modules, but in particular there have been very few attempts at recovering the copper in the photovoltaic modules.<sup>5)</sup>

Existing copper recovery methods involve oxidizing the copper ribbon electrode at high temperatures of 800°C or more in order to separate the oxidized coating layer from the base material. However, in this study a water oxidation method at a lower temperature of 500°C is used for oxidation, and a ball milling process is subsequently carried out in order to separate the oxidized coating layer from the base material. The recovered copper base is analyzed by ICP-MS (inductively coupled plasma mass spectrometry), and the oxidized coating layer is analyzed using XRF (X-ray fluorescence) and XRD (X-ray diffraction).

## 2. Methods and Materials

### 2.1 Experimental Setup

Figure 1 shows the experimental setup used in this study, which includes an electric furnace, a thermocouple and a heater, as well as a tube that connects a flask containing distilled water and the electric furnace for the injection of H<sub>2</sub>O. To prevent the water vapor from condensing in the tube, the tube was wound with heating tape.

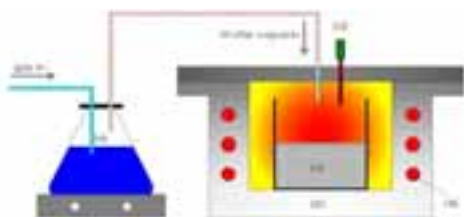


Fig. 1 Schematic of H<sub>2</sub>O oxidation process (a: distilled water, b: furnace, c: photovoltaic ribbon, d: thermocouple, e: heater)


Figure 2 is an image of the ball milling equipment, which was used to oxidize the copper ribbon during the H<sub>2</sub>O oxidation process and to separate the copper base from the oxidized coating layer, as well as an image of the milling balls used in the test.



Fig. 2 Ball milling equipment and used milling balls

Three 30mm diameter balls and 15 0.7mm diameter balls were used in the test.

Table 1. Chemical composition of photovoltaic ribbon analyzed by ICP-MS

	Element	Weight, %
	Cu	87.752
	Pb	5.247
	Sn	6.150
	Nb	0.063

	Ag	0.046
--	----	-------

## 2.2 Test Materials

The chemical composition of the photovoltaic ribbon of KOSBON Co. used as the test material is given in Table 1. Based on the ICP-MS results, the ribbon contained 87.752% copper, 5.427% lead, 6.150% tin and trace amounts of niobium and silver.

## 3. Results

The spent photovoltaic module was heat treated under air condition at 500°C for 2h to recover the copper ribbon electrode from the module. The coating layer was then oxidized to separate and recover the copper base and the scale under the following reactions.



Table 2 shows the thermodynamic properties for the oxidation reactions of copper, lead and tin, the main components of the copper ribbon electrode, as determined by HSC Chemistry<sup>5,1</sup>.

Copper, lead and tin underwent forward reactions because their  $\Delta G$  values were less than 0, as shown in the Table 2, confirming activated oxidation reactions.

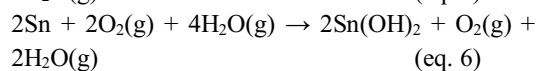
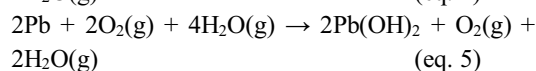
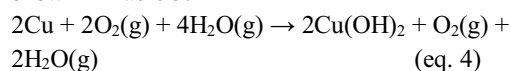
Table 2 Thermodynamic properties of oxidation reactions of copper, lead, and tin

<b>2Cu + O<sub>2</sub>(g) = 2CuO</b>			
T	$\Delta H$	$\Delta S$	$\Delta G$
C	Kcal	cal/K	Kcal
0	-74.504	-44.552	-62.335
100	-74.308	-43.955	-57.906
200	-73.987	-43.196	-53.548
300	-73.612	-42.479	-49.265
400	-73.211	-41.834	-45.05
500	-72.795	-41.258	-40.896

<b>2Pb + O<sub>2</sub>(g) = 2PbO</b>			
T	$\Delta H$	$\Delta S$	$\Delta G$
C	Kcal	cal/K	Kcal
0	-104.285	-47.342	-91.354
100	-104.056	-46.631	-86.655

200	-103.778	-45.974	-82.026
300	-103.483	-45.408	-77.457
400	-105.494	-48.774	-72.662
500	-105.154	-48.303	-67.808
<b>2Sn + O<sub>2</sub>(g) = 2SnO</b>			
T	ΔH	ΔS	ΔG
C	Kcal	cal/K	Kcal
0	-134.256	-46.427	-121.574
100	-133.974	-45.544	-116.979
200	-133.732	-44.968	-112.455
300	-136.901	-51.263	-107.52
400	-136.543	-50.689	-102.422
500	-136.124	-50.11	-97.382

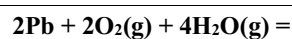
The chemical equations for the reactions of copper, lead and tin with oxygen and H<sub>2</sub>O are shown below, and the thermodynamic properties of these reactions (as determined using HSC chemistry) are shown in Table 3.



The copper, lead and tin that reacted with oxygen and H<sub>2</sub>O also showed forward reactions because their ΔG values were less than 0, as shown in Table 3, confirming activated oxidation reactions. Based on these theoretical values, the oxidation test temperature was set to 500°C.

**Table. 3 Thermodynamic properties of reactions of copper, lead, and tin with oxygen and H<sub>2</sub>O**

<b>2Cu + 2O<sub>2</sub>(g) + 4H<sub>2</sub>O(g) = 2Cu(OH)<sub>2</sub> + O<sub>2</sub>(g) + 2H<sub>2</sub>O(g)</b>			
T	ΔH	ΔS	ΔG
C	Kcal	cal/K	Kcal
0	-72.759	-47.729	-59.722
100	-77.249	-63.331	-53.617
200	-78.623	-66.593	-47.115
300	-80.327	-69.837	-40.3
400	-83.17	-74.398	-33.089
500	-86.065	-78.409	-25.443



<b>2Pb(OH)<sub>2</sub> + O<sub>2</sub>(g) + 2H<sub>2</sub>O(g)</b>			
T	ΔH	ΔS	ΔG
C	Kcal	cal/K	Kcal
0	-129.511	-125.142	-95.329
100	-133.117	-136.384	-82.226
200	-136.83	-145.193	-68.132
300	-140.663	-152.538	-53.235
400	-146.934	-162.752	-37.378
500	-150.982	-168.357	-20.816
<b>2Sn + 2O<sub>2</sub>(g) + 4H<sub>2</sub>O(g) = 2Sn(OH)<sub>2</sub> + O<sub>2</sub>(g) + 2H<sub>2</sub>O(g)</b>			
T	ΔH	ΔS	ΔG
C	Kcal	cal/K	Kcal
0	-151.72	-86.529	-128.085
100	-155.35	-97.843	-118.84
200	-159.122	-106.791	-108.594
300	-166.418	-120.996	-97.069
400	-170.307	-127.25	-84.649
500	-174.258	-132.72	-71.645

First, to oxidize the coating layer through the use of water vapor, distilled water is placed in the flask connected to the furnace and boiled. In order to facilitate the injection of water vapor into the furnace, argon gas was injected into the flask at 100 cc/min. After inserting the heat-treated copper ribbon into a furnace for 2h, the ribbon was heat treated at 500°C in order to facilitate the oxidation test. The original copper ribbon sample used in the test weighed 15g, and the H<sub>2</sub>O oxidation tests were carried out at time intervals of 1, 3, 5 and 10 hrs. The oxidized copper was analyzed by SEM (scanning electron microscopy) to analyze the oxidized layer. Figure 3 shows images of the oxidized copper ribbons for each reaction time.

Afterwards, the copper base was recovered by ball milling at 90rpm for 1h and was analyzed by ICP-MS, and the oxidized coating layer was analyzed by XRF and XRD.



Fig. 3 H<sub>2</sub>O oxidized photovoltaic ribbons(a: 1 h; b: 3 h, c: 5 h, d: 10 h)

4. Discussion

Rather than using the existing high temperature oxidation approach under atmospheric conditions at 800°C to recover copper from the copper ribbon electrode in the spent photovoltaic module, an H<sub>2</sub>O oxidation approach was carried out at 500 °C for 1 h, 3h, 5h, and 10h. The weight of the oxidized copper ribbon increased by 0.32g after 1h H<sub>2</sub>O oxidation, by 0.53g after 3h oxidation, by 0.98g after 5h oxidation, and by 1.20g after 10h oxidation. The amounts of distilled water consumed were 551.17g, 891.52g, 1673.24g, and 3172.48g, respectively. To compare the weight change between the air and H<sub>2</sub>O oxidation tests under atmospheric conditions, an air oxidation test was carried out under atmospheric conditions, similar to the H<sub>2</sub>O oxidation test, and the copper ribbon was heat treated for 1h, 3h, 5h, and 10h at 500 °C. The weight of the copper ribbon increased by 0.054g after 1h heat treatment, by 0.16g after 3h heat treatment, by 0.36g after 5h heat treatment, and by 0.38g after 10h heat treatment. Figure 4 shows the comparison of weight increases between the H<sub>2</sub>O atmosphere oxidation and air atmosphere oxidation methods. As the graph shows, the weight increases from the H<sub>2</sub>O method were much greater than those of the air atmosphere method, with the oxidized amount sharply increasing after 3h.

Figure 5 shows the SEM results of the coating layer of the H<sub>2</sub>O oxidized copper ribbon. The left-most photo shows the coating layer of the copper ribbon before the oxidation test, where the lead and tin coating layers have thicknesses of 20µm and the thickness of the coating layer of the copper ribbon is 50µm after 1h H<sub>2</sub>O oxidation, 160µm after 3h H<sub>2</sub>O oxidation, 155 µm after 5h H<sub>2</sub>O oxidation, and 146µm after 10h H<sub>2</sub>O oxidation. These results confirm rapid oxidation after 1h of oxidation, which

greatly increased the thickness of the oxidized

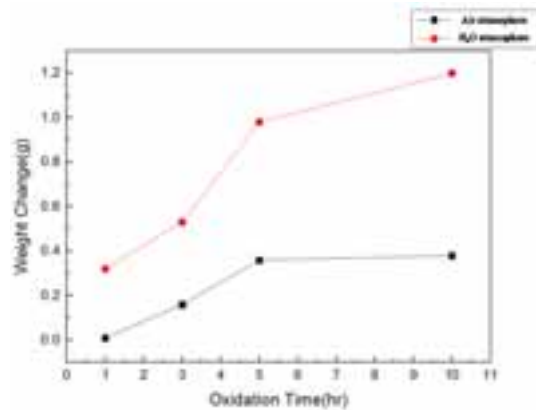


Fig. 4 Weight increases of air atmosphere and H<sub>2</sub>O atmosphere oxidation conditions.

coating layer. After 5h, the copper base and the oxidized coating layer were separated. The oxidized copper ribbon electrode was separated into the copper base and oxidized coating layer by ball milling.

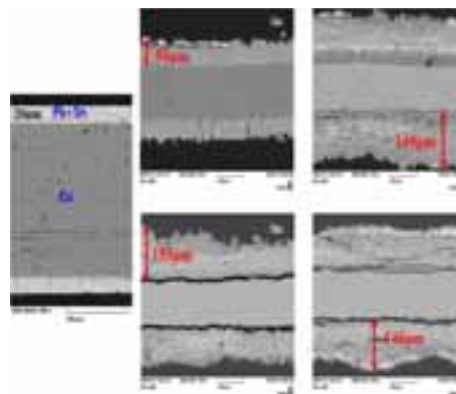


Fig. 5 Coated layer of oxidized photovoltaic ribbon sample analyzed by SEM

Table 4. Weight increase after H<sub>2</sub>O oxidation and recovered oxide scale weight after ball milling process

Oxidation time, hr	Weight increase	Recovered oxide scale weight
1	0.32 g	0.35 g
3	0.53 g	1.53 g
5	0.98 g	5.94 g
10	1.20 g	6.54 g

Table 5. The recovered copper ribbon analyzed by ICP-MS

500 °C – 5 hours		800 °C - 30 mins	
Element	weight %	Element	weight %

Cu	98.106	Cu	99.554
Pb	0.992	Pb	0.027
Sn	0.716	Sn	0.297
Nb	0.065	Nb	0.071
Ag	0.003	Ag	0.009

Pb	10.91	Pb	10.21
Cl	2.01	Cl	1.94
Zn	0.49	Zn	0.38
Si	0.47	Si	0.21
Al	0.16	Al	0.08

Figure 6 shows the copper base and oxidized coating layer separated by ball milling, and Table 4 shows the weight increase after H<sub>2</sub>O oxidation and the weight of the oxidized scale recovered by the ball milling process for each oxidation time. As shown in the table, 0.35g, 1.53g, 5.94g, 6.54g of



Fig. 6 The recovered copper ribbon and the oxide scale (a: 1 h; b: 3 h, c: 5 h, d: 10 h)

oxide scale were recovered at oxidation times of 1h, 3h, 5h, and 10h, respectively, and the amount of recovered oxide scale greatly increased after 5 h of oxidation time, indicating oxidation of most of the copper coating layer in the copper ribbon electrode at this point, allowing for good separation of the copper base and the copper coating layer. ICP-MS analysis of the recovered copper base showed that 98.106% pure copper could be obtained, and this result is compared to that of the 800 °C oxidized copper base in Table 5. The recovered oxide scale was analyzed by XRF and XRD and the results are shown in Table 6 and Fig. 7.

Table. 6 XRF data from the recovered oxide scale

500 °C – 5 h		500 °C – 10 h	
Element	Weight %	Element	Weight %
Cu	68.21	Cu	70.40
Sn	17.72	Sn	16.74

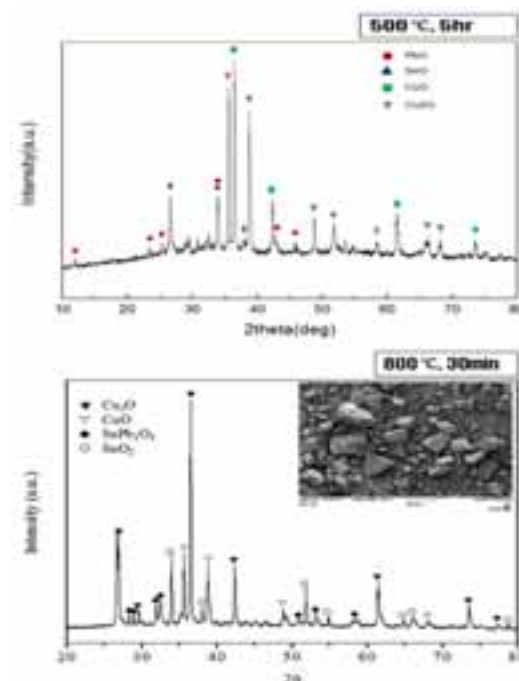


Fig. 7 The recovered oxide scale analyzed by XRD

### 5. Conclusions

Rather than using the existing high temperature oxidation method at 800°C in atmospheric conditions to oxidize copper ribbon electrodes for the separation of the base material from the oxide coating layer, this study used a H<sub>2</sub>O oxidation method at 500°C, and the oxidized copper ribbon electrode was ball-milled to separate the base material from the oxide coating layer. The following results were obtained from the separation test:

- (1) Based on the SEM results of the copper ribbon oxidized using the H<sub>2</sub>O method at 500°C, the thickness of the coating layer of the copper ribbon was 50 μm after 1 h H<sub>2</sub>O oxidation, 160 μm after 3h H<sub>2</sub>O oxidation, 155μm after 5h H<sub>2</sub>O oxidation, and 146 μm after 10h H<sub>2</sub>O oxidation, with the oxidation proceeding more rapidly after 1h to greatly increase the thickness of the oxide coating layer, resulting in the separation of the copper base from the oxide coating layer after 5 h.
- (2) Based on comparisons of the weight increase between H<sub>2</sub>O oxidation and air atmosphere

oxidation at 500°C, the weight increase of the H<sub>2</sub>O oxidized copper ribbon was about 3 times that of the copper ribbon oxidized by air atmosphere oxidation, confirming that more efficient oxidation is achieved with the water vapor method.

- (3) After ball-milling to separate the copper base from the oxide coating layer, the weight of the recovered oxide scale was measured. 0.35g, 1.53 g, 5.94g and 6.5g of oxide scale could be recovered after oxidation times of 1h, 3h, 5h, and 10h, respectively.
- (4) The ICP-MS analysis results of the recovered copper base after ball-milling showed that the purity of the recovered copper base was 98.106%, which was similar to that of the recovered copper base oxidized at 800°C.
- (5) XRF and XRD analysis revealed that the recovered oxide scale contained 68.21% copper, 17.72% tin and 10.01% lead, all existing as oxides.

### **Acknowledgements**

This work was supported by the Korea Institute of Energy Research (No. GP2012-0001-08).

### **Reference**

1. Lee. J. S., Wang. J. P., Lee. W. J., Kim. Y. H., Jung. W. C., 2014. Study on fabrication of high purity copper from spent photovoltaic ribbon in solar module, *Journal of Korean Inst. of resources recycling*, pp. 33-37.
2. Max, M., Wolfgang, B., Martin, S., Andreas, M., Armin, R., 2013. Recycling paths of thin-film chalcogenide photovoltaic waster-Current feasible processes, *Renewable Energy*, 55, pp. 220-229.
3. Bruton, T.M., 1995. Production of high efficiency monocrystalline silicon solar cell, *Renewable Energy*, 6, pp. 299-302.
4. Fthenakis, V.M., 2000. End-of-life management and recycling of PV modules, *Energy Policy*, 20, pp. 1051-1058.
5. Lee. J. S., Jang. B. Y, Kim. J. S., Ahn. Y. S., Kang. G. H., Wang. J. P., 2013. Recovery of copper from spent photovoltaic ribbon in solar module, *Journal of Korean Inst. of resources recycling*, Vol.22, No.5, pp. 50-55.